

A repeating earthquake catalog for Northern Chile

Jonas Folesky  *¹, Jörn Kummerow , Laurens Jan Hofman 

¹Department of Geophysics, Freie Universität Berlin, Berlin, Germany

Author contributions: *Conceptualization:* J. Folesky, J. Kummerow. *Methodology:* L. J. Hofman, J. Folesky. *Software:* L. J. Hofman, J. Folesky. *Formal analysis:* J. Folesky, L. J. Hofman. *Writing - original draft:* J. Folesky. *Writing - review & editing:* J. Folesky, J. Kummerow. *Visualization:* J. Folesky. *Funding acquisition:* J. Folesky.

Abstract Repeating earthquakes are nearly identical seismic events that are assumed to occur reiteratively on the same fault-patch with highly consistent focal mechanisms. Their magnitude-dependent recurrence intervals can be used to estimate local fault-slip and to infer spatial and temporal patterns of aseismically creeping zones at depth. We construct here the first long-term repeating earthquake catalog for Northern Chile. Using waveforms for 180 000 earthquakes from a recent regional seismicity catalog as templates, a GPU-based template matching is performed to search for repeating earthquakes in the continuous, multiannual seismological data of the permanent IPOC station network between 2006 and 2024. The resulting repeater catalog contains 10 684 events grouped into 3153 families. We observe a notable variability of size and behavior of the families, ranging from long-lasting, regular sequences to short-term, burst-type repeaters. Two megathrust earthquakes in 2007 and 2014 have a strong effect on the spatio-temporal distribution of repeaters. We compute the first time-dependent slip map for the interface between the subducting Nazca slab and the overriding South American plate. The catalog facilitates future detailed analysis of rupture processes, source structures and the spatio-temporal evolution of slow slip at depth. It also allows for comparative studies with other subduction zones, such as Japan.

Production Editor:
Andrea Llenos
Handling Editor:
Mathilde Radiguet
Copy & Layout Editor:
Abhineet Gupta

Signed reviewer(s):
Blandine Gardonio

Received:
January 1, 2025
Accepted:
July 21, 2025
Published:
August 8, 2025

1 Introduction

The occurrence of repeating earthquakes (REs), or repeaters, has been well documented for many regions of the world and for various tectonic settings (cf. reviews by Uchida, 2019; Uchida and Bürgmann, 2019). They are conceived as seismic events which rupture repeatedly the same fault area, have nearly identical mechanisms and therefore exhibit highly similar waveforms (Menke, 1999). The prevalent model to explain repeaters is that of an identical, reiteratively activated slip patch of a strong asperity, which is surrounded by or adjacent to a region of aseismic creep, that consistently loads the locked asperity, enforcing repeated seismic energy release (e.g., Nadeau and Johnson, 1998; Matsuzawa et al., 2014; Chen et al., 2010). Therefore, repeaters are considered as tracers for the slip of their local aseismic environment at depth.

The special characteristics of REs allow their utilization for various purposes. Their recurrence intervals, for example, have been used to test earthquake predictability (Nadeau and Johnson, 1998; Uchida and Bürgmann, 2019), their spatio-temporal evolution to characterize after-slip (Kato et al., 2016; Uchida and Bürgmann, 2021), and their long-term source stability to study temporal changes of the local velocity structure (Rubinstein et al., 2007; Chen et al., 2011); importantly, they have also been used to infer inter-plate aseismic slip at depth (e.g., Igarashi, 2010; Kato et al., 2016; Uchida, 2019).

Identification of RE sequences is commonly achieved by computing the waveform cross correlation as a measure of waveform similarity (e.g., Igarashi et al., 2003). This is applied to search for similar events within an event catalog or by a template matching (also called match filter) technique, where the waveform of a given event is used as a template to search for similar events (matches) within the continuous seismic recordings. While repeaters are understood to represent ruptures of identical or at least overlapping patches of the same fault, their practical identification is less well defined. Hence, parameter thresholds and criteria for defining repeaters differ between authors (Gao et al., 2021). In addition to or instead of using measures of waveform similarity, some studies also use relative event location techniques or directly differential $T_S - T_P$ travel times to estimate the distance between their hypocenters, and force the RE to have overlapping fault patches (Uchida, 2019). This approach additionally requires estimates of the event magnitudes and also of stress drops, which are commonly not calculated and fixed to a standard value (e.g., 3 MPa). The estimated fault dimensions, required to assess the potential source overlap, are also sensitive to the utilized source model.

A few studies have previously identified and investigated repeating earthquakes in Northern Chile, but with a clear focus on the surrounding area of the 2014 Iquique $M_w 8.1$ megathrust earthquake and its fore-shock and after-shock series (Meng et al., 2015; Kato et al., 2016; Soto et al., 2019).

In this work, we make use of the entire continuous

*Corresponding author: jonas.folesky@geophysik.fu-berlin.de

seismological recordings of the Integrated Plate boundary Observatory Chile ([GFZ German Research Centre For Geosciences and Institut Des Sciences De L'Univers-Centre National De La Recherche CNRS-INSU, 2006](#)) which has been active since 2006 and which is located between 18°S and 24°S. Its relative stability allows the search for repeaters during the observation period from 2006 to 2024. The study region is strongly dominated by the subduction of the Nazca plate below the South American plate. The full seismicity catalog of [Sippl et al. \(2023a\)](#) is used to extract template waveforms for ~180 000 events and then perform template matching for the continuous waveform data.

We identify several thousands of repeater series with a wide range of recurrence patterns and in different parts of the subduction zone. We label and classify them according to their duration and variation of recurrence behavior, and we thereby aim to provide a solid basis for subsequent repeater based analysis in the future.

In a last step, we provide the yearly slip-rate maps computed from averaging the RE derived slip-rates.

2 Seismicity data

This study is based on the seismological broadband data from the Integrated Plate Observatory Chile ([GFZ German Research Centre For Geosciences and Institut Des Sciences De L'Univers-Centre National De La Recherche CNRS-INSU, 2006](#)) in North Chile. Established in 2006, the network provides publicly available continuous records from its permanent stations and several temporary deployments. Here, we use the 100 Hz vertical component (HHZ) waveform data obtained by the broadband instruments from the permanent CX-net. The analyzed time period is from 2006 to 2024. The recent IPOC seismicity catalog by [Sippl et al. \(2023a\)](#), which encompasses over 180 000 events between 2007 and 2021, defines the template events for constructing the repeating earthquake catalog. Although the catalog ends in 2021, the template matching was performed for the entire waveform data from late 2006 to the end of 2024. An overview of the data availability of the 5 to 25 stations can be found in the electronic supplement (Figure S1). Station locations are shown in Figure 1 & Figure S2.

3 Method

To search for repeating earthquakes in the entire continuous IPOC waveform data, we apply our own template matching procedure as described in [Hofman et al. \(2023\)](#), which was also previously used in Northern Chile to find empirical Green's functions for stress drop mapping ([Folesky et al., 2024](#)). The code is GPU-based and applies matrix multiplication for fast computation of the cross-correlation in the frequency domain using CuPy, a Python library for GPU-accelerated computing ([Okuta et al., 2017](#)). Here, we use a single Nvidia GV100 graphics processing unit (GPU) with 8192 cores. Albeit computationally expensive, the event search applied to the entire continuous seismogram recordings instead of

only cross correlating the cataloged events proves to be important for the completeness of the resulting RE catalog. In our study, 51.6 % of the finally detected REs were not part of the original IPOC catalog, i.e., about half of the events would not have been captured without the exhaustive search in the continuous waveform data, which would have compromised completeness significantly.

For the template matching, recordings of all 180 000 earthquakes in the IPOC catalog are used as templates. Although this is computationally intensive, we prescind from pre-clustering the events in order to capture the RE sequences as completely as possible. In the first iteration, vertical component seismograms are extracted for each template at the three closest available stations. The width of the extracted time window is chosen variable, dependent on the source receiver distance. The minimum length of the template waveform is set to 15 s, and it is extended with hypocentral distance to ensure that the time window always contains both the P and S phases. Seismograms are 1–4 Hz band-pass filtered and downsampled to 25 Hz. Preliminarily, we require the absolute, normalized cross correlation coefficient (cc) to exceed a value of cc=0.85 at minimum two stations to define a potential repeater detection candidate. In the second iteration, we then use all new potential RE candidates from the first iteration as templates for the template matching. Here, we extend the number of stations to the five closest stations in order to improve the detectability and enhance the completeness of the repeater families. We finally define RE families as groups of events, where each event has an absolute cc value of cc≥0.95 with at least one other event of the family at minimum two stations. We accept high similarity on only two stations here because of the relative sparsity of the station network, in particular during the early stage of the network deployment. We therefore decided not to extend these requirements to three or more stations, because it turned out that, for instance, we then missed a significant portion of events in RE sequences with clearly periodic behavior. On the other hand, we found no indication of introducing spurious repeating events by using only 2 stations. Note, that the applied criteria, using a frequency band of 1–4 Hz, a high cc threshold of cc≥0.95 and the long time window including both P and S phases, are comparatively strict ([Uchida and Bürgmann, 2019](#); [Gao et al., 2021](#)). We decided not to include the inter-event distance as an additional constraint for co-location of the events, because the location uncertainty is of the order of a few kilometers ([Sippl et al., 2023a](#)), which is significantly larger than most of the estimated source dimensions. The largely deep and/or offshore seismicity and the comparatively sparse station geometry also complicate here the otherwise often effective reduction of location errors by application of relative relocation methods.

In the resulting RE catalog, each new detection inherits the location of its template. Events, which were already part of the IPOC catalog and which are grouped together by high cc values, keep their original location.

For each event of a RE sequence, we estimate the slip by using the empirical slip-to-moment relation originally introduced by [Nadeau and Johnson \(1998\)](#) for re-

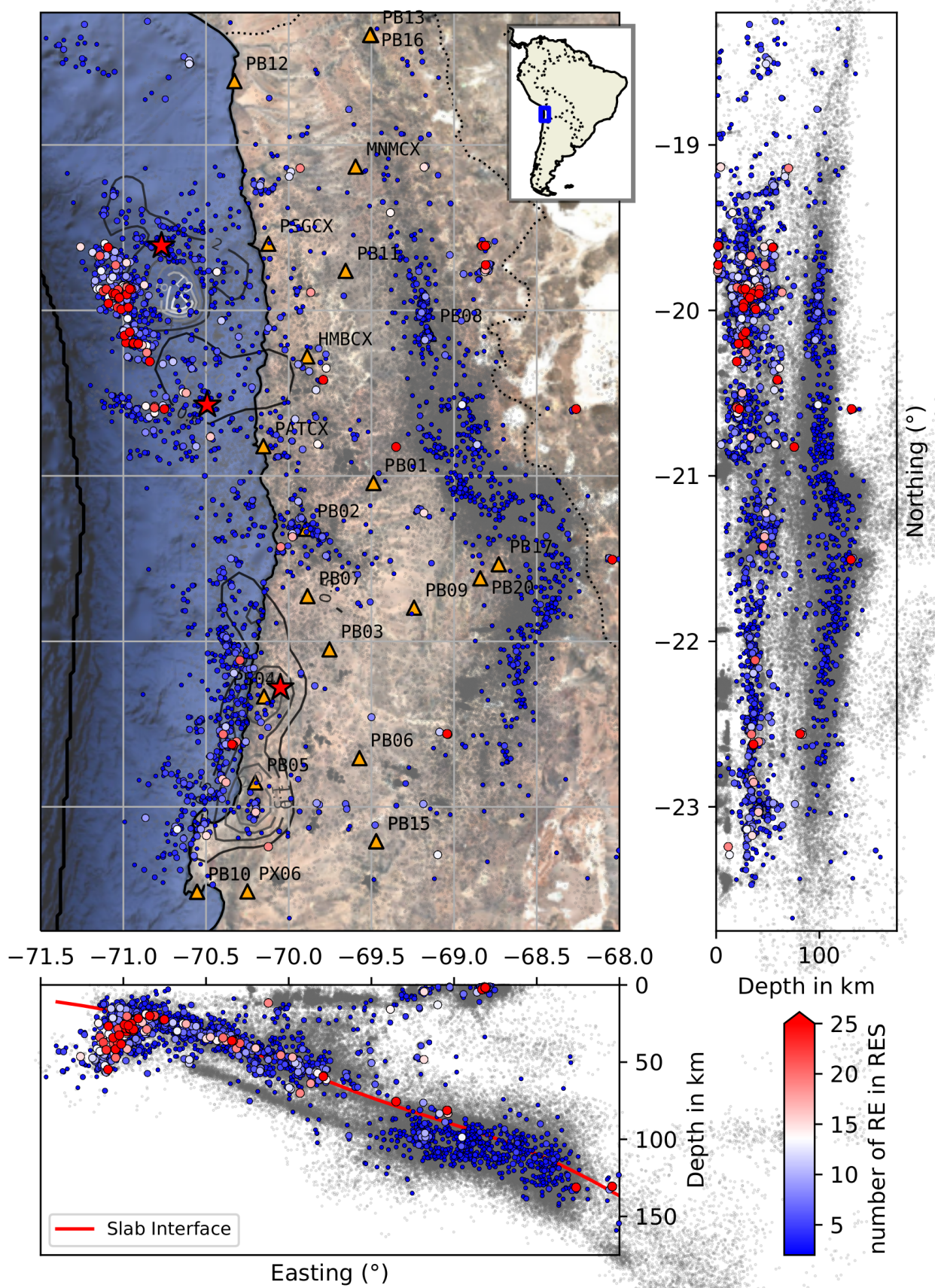


Figure 1 Locations of repeating earthquake sequences (RES) in the target region. Color indicates the number of family members. Orange triangles are IPOC station locations. The background seismicity shown in gray is taken from Sippl et al. (2023b). From north to south, red stars are the hypocenters of the 2014 $M_w 8.1$ Iquique earthquake, its $M_w 7.7$ after-shock, and the 2007 $M_w 7.7$ Tocopilla earthquake. Note that most of the RES with multiple members are located close to the plate interface. They agglomerate up-dip of the coseismic slip patches (Schurr et al., 2012, 2014; Duputel et al., 2015) of the large megathrust events. Slab is taken from Sippl et al. (2018).

peaters in Parkfield, CA, US.:

$$\log(d) = -2.36 + 0.17 \log(M_0), \quad (1)$$

where the slip d is in cm and the seismic moment M_0 is in dyne-cm. The cumulative slip is simply obtained by summing over all events in the sequence. The relation by Nadeau and Johnson (1998) has been shown to be robust for repeaters in various different regions, in particular subduction zone settings such as the Japanese islands (Igarashi, 2010, 2020), New Zealand (Hughes et al., 2021), and Taiwan (Chen et al., 2008), suggesting that it is also applicable in our study region in Northern Chile, where it was already used earlier by Meng et al. (2015).

The seismic moment M_0 in Eq. 1 is estimated from the magnitudes provided in the original IPOC catalog (Sippl et al., 2023b). The therein defined magnitudes labeled M_A are considered as moment magnitudes M_w , similar as in Folesky et al. (2024), and we use the relation $M_w = \frac{2}{3}(\log_{10} M_0 - 9.1)$ (Hanks and Kanamori, 1979) to convert the magnitudes to the seismic moment M_0 in N-m. For newly detected repeaters, which are not contained in the original catalog, we compute the amplitude ratio of the detected event to the template event, and average over the available stations. The magnitude for the detected event is then determined as

$$M_{\text{detection}} = \log_{10}(A_{\text{detection}}/A_{\text{template}}) + M_{\text{template}}. \quad (2)$$

We verified the validity of this approach as described in Figure S3 in the supplement.

4 Results

We found 10 684 events in 3153 RE sequences in the study region in North Chile between 18°S and 24°S for the analyzed time period from late 2006 to the end of 2024. Their spatial distribution is shown in Figure 1, where the location of each RE family is represented by its geometric median. Repeaters are observed at the plate interface, but also in the continental crust of the upper plate, in the double seismic zone within the subducting slab, and at intermediate depth. The overall percentage of REs in the IPOC cataloged seismicity is $n_{\text{RE}}/n_{\text{cat}} = 5192/182841 = 2.8\%$, where the newly detected REs ($n=5492$) are not considered. For the different tectonic settings, the relative number of repeaters varies considerably. Following the definition of event classes in the IPOC catalog (Sippl et al., 2023b), the percentages of REs compared to total IPOC event counts are: 15.6 % for interface seismicity, 3.1 % for upper plane seismicity, 0.4 % for lower plane seismicity, 4.4 % for seismicity in the continental crust of the upper plate, and 1.1 % for intermediate depth seismicity, respectively. Additionally, we found that a considerable number of mining events meet our criteria for repeaters. The number of mining events that formally classify as REs is 1292, from which 686 were cataloged in the IPOC catalog, which translates into 4.1 % of the mining events in the IPOC catalog. They are not included in the repeater catalog and the above event count, but we provide a list of them in a separate file (see data section).

The event distributions of the RE families and their magnitude distributions are shown in Figures 2 & 3,

respectively. Most families are doublets and triplets ($n_{\text{fam}_{n=2}}=2105$, $n_{\text{fam}_{n=3}}=471$), but there exist numerous larger families ($n_{\text{fam}_{n>3}}=576$) which are interesting for further analysis.

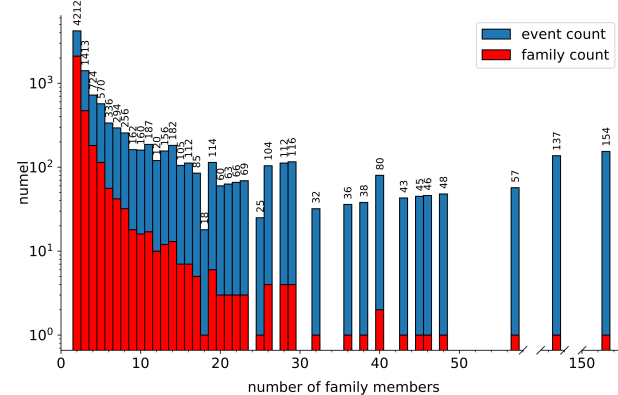


Figure 2 Histogram of number of individual RE events (blue) and number of RE families of a given family size (red). E.g., there exists one family (red bar count = 1) with 137 members (blue bar count = 137), but three families each with 20 members with a total of 60 events. Note the broken x-axis for better visualization.

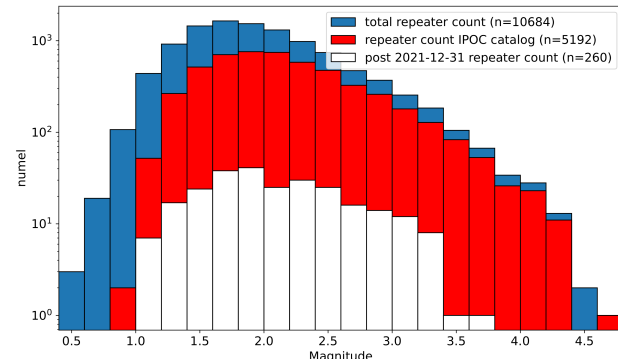


Figure 3 Histogram of magnitudes in the repeater catalog. Blue bars indicate event counts for the entire catalog. Red bars show only those repeaters that were already part of the IPOC catalog. White are repeating events that were detected in the years 2022–2024 which were not covered by the IPOC catalog anymore, but still yielded repeater matches.

Exemplarily, waveforms for two repeating earthquake families, fam_{cID62} consisting of 13 events and fam_{cID2426} consisting of 18 events, are illustrated in Figures 4 & 5, together with their median locations and estimated cumulative slip history using Eq. 1 to determine the slip for each event. In the second series (Figure 5d), there is apparently one event missing in 2018–2019, due to data gaps at the two nearby stations PSGCX and PB11 here. In general, we aimed at minimizing the number of missing events by requiring the $\text{cc} \geq 0.95$ criterion for only two stations and by applying the template matching to the complete continuous waveform data. Note that for this series, 5 out of 18 events are newly detected events which were not listed in the original IPOC catalog. Both series are located at similar

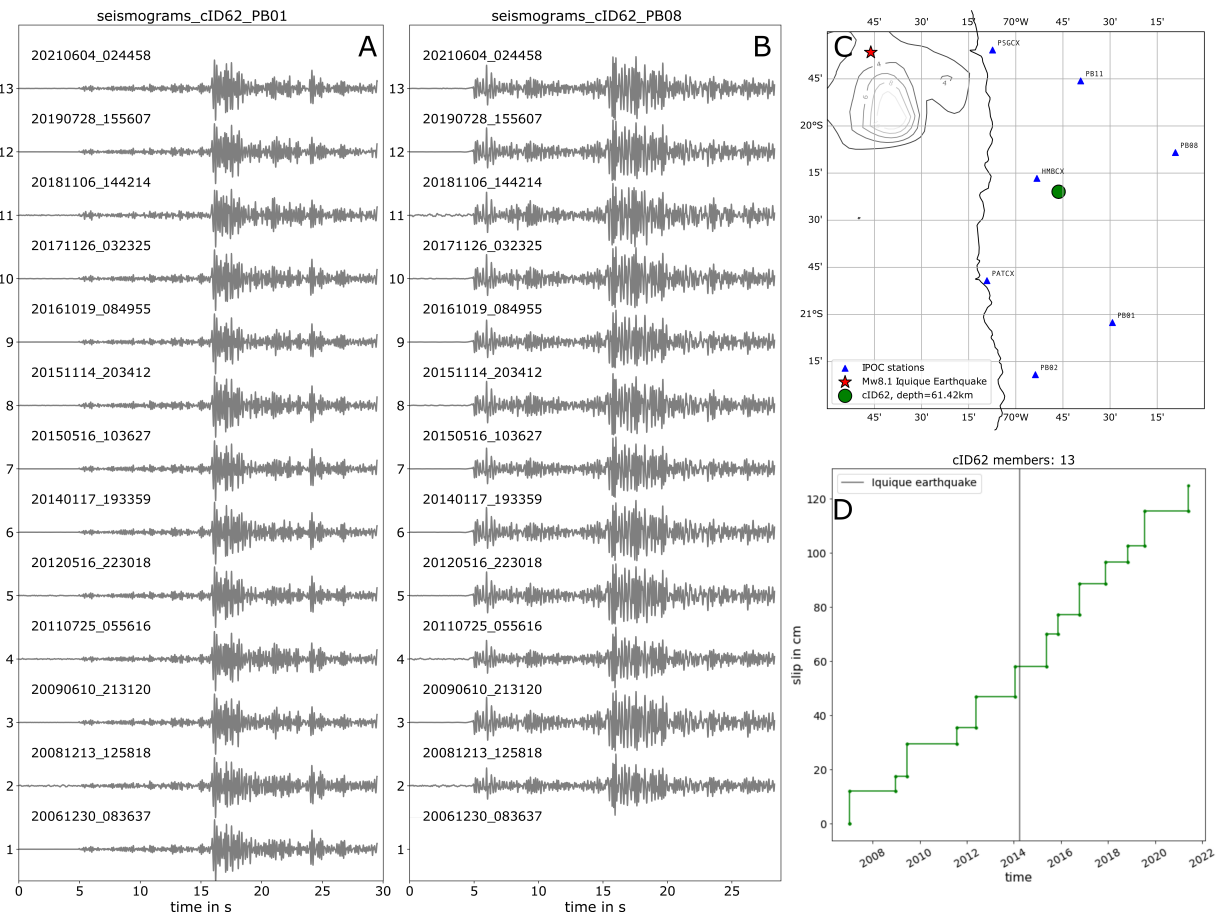


Figure 4 Repeating earthquake family 62. For this family, 13 members were detected. A and B show z-component velocity waveforms filtered between 1–8 Hz from stations PB01 and PB08, respectively. The displayed time window starts 5 seconds before the p pick and continues for twice the $T_S - T_P$ differential time. C shows the family location and D displays slip vs. time.

Note the remarkable similarity between the events. The seismic activity of the family is continuous and the slip-rate remains constant over time, while family members may exhibit variable slip, i.e., have different magnitudes. This family appears completely unaffected by the 2014 Iquique event (red star in C and vertical line in D).

depth of about 60 km, but the second series lies further north and closer to the rupture area of the 2014 $M_w 8.1$ Iquique event (red star and slip-isolines in Figures 1, 4, and 5). While fam_{cID62} shows a fairly constant average slip-rate and was observed continuously during the recording period from the beginning in the year 2006 on, fam_{cID2426} initiated 2 weeks after the main shock in April 2014. In its early phase, it exhibits short recurrence intervals which extend progressively with time and result in a temporal decay of the slip-rate (cf. Figures 4d & 5d) until an approximately constant slip-rate is reached, which is still ongoing. The Iquique megathrust event apparently initiated the series, modulated temporarily the stress field and induced time-dependent after-slip in the area of the repeater asperity.

As demonstrated by the two families, the resulting RE catalog encompasses sequences with a range of temporal characteristics, several of which have a more complex recurrence behavior than the examples shown. To classify all the series, we use their total duration, which is the time between the first and last events, the standard deviation of magnitude (M_{std}), and we compute the coefficient of variation of the recurrence time (cv_r) after

Waldhauser and Schaff (2021):

$$cv_r = \frac{\sqrt{\frac{1}{N-1} \sum_{i=2}^N (T_{ri} - \bar{T}_r)^2}}{\bar{T}_r} \quad (3)$$

Here N is the number of REs in the repeater sequence, T_{ri} is the recurrence time between events, and \bar{T}_r is the average recurrence time. Additionally, using the above measure, we categorize all series that have more than three members into recurrence types in the following way:

qp - quasi periodic - are series with nearly periodic behavior. They must have a coefficient of variation of $cv_r < 0.75$ and the standard deviation of their magnitudes must obey $M_{std} < 0.55$.

bu - burst - are series that have a short total duration of less than one year.

dc - decay - are series which show an Omori type decay in their recurrence behavior which is expressed by consecutive increase of the recurrence time between events.

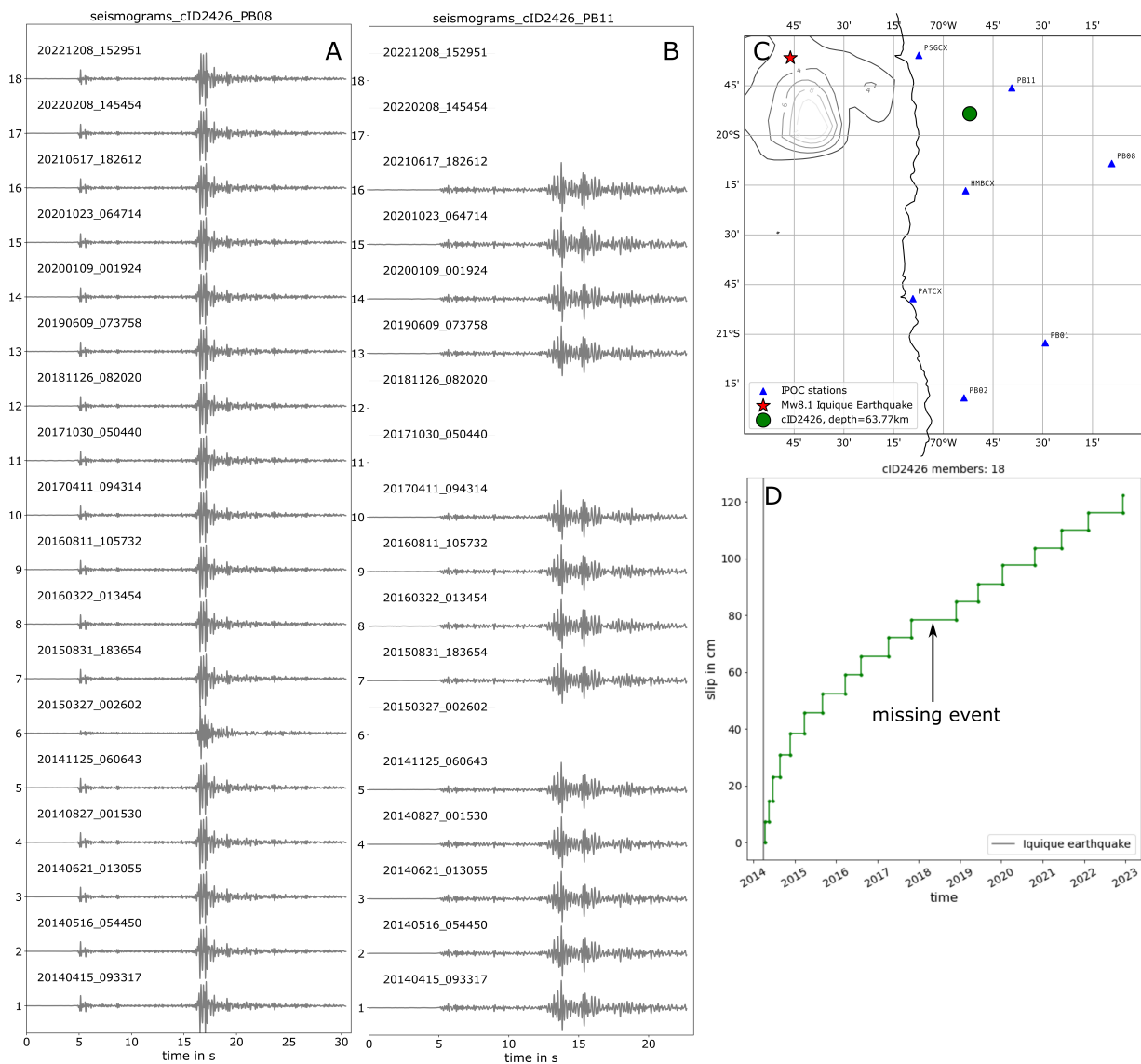


Figure 5 Repeating earthquake family 2426. For this family, 18 members were detected. A and B show z-component velocity waveforms filtered between 1–8 Hz from stations PB08 and PB11, respectively. C shows the family location and D displays slip vs. time.

Note the difference in the time axis compared to Figure 4. The seismic activity of the family started just after the Iquique event, and it is continuous. The average slip-rate decreases rapidly (i.e., the inter-event waiting time increases) in the first three years after occurrence until it stabilizes onto a linear slope. Family members exhibit little variations in slip, i.e., have similar magnitudes which decrease slightly over time. This family appears heavily affected by the 2014 Iquique event (red star in C and vertical line in D) very much in contrast to series cID62 in Figure 4. Note the suspiciously long inter-event gap in 2018–2019 in D. It is likely that one event is missed here, because of missing data from station PSGCX and PB11 in that time window.

rb - repeated burst - are series which show at times burst behavior, which is the repeated rapid recurrence of REs within a time period of days to weeks, followed by a longer waiting time, until a new burst phase initiates.

ap - aperiodic - are series which show higher than qp-type cV_r , and do not fall into any of the other categories.

For few series, multiple recurrence type labels are assigned if their behavior fulfills multiple criteria. Each recurrence curve was double-checked manually following the initial automated classifier to resolve the more complex cases. Note that the classification is based on

rather arbitrary parameters and small shifts may lead to different type associations. Nevertheless, the assigned types may help to better preselect subgroups of repeating sequences for subsequent research.

The recurrence type classification, applied to the 578 families with $n > 3$ members, results in 193 qp-labels, 139 bu-labels, 308 dc-labels, 21 rb-labels and 109 ap-labels. We plot their spatial distribution in Figure S10 in the supplement.

The assigned parameters provide a means to find and extract more easily specific RE groups. For example, there exist several RE sequences that exhibit the high waveform similarity required for repeater families, but most likely are not classical repeaters associ-

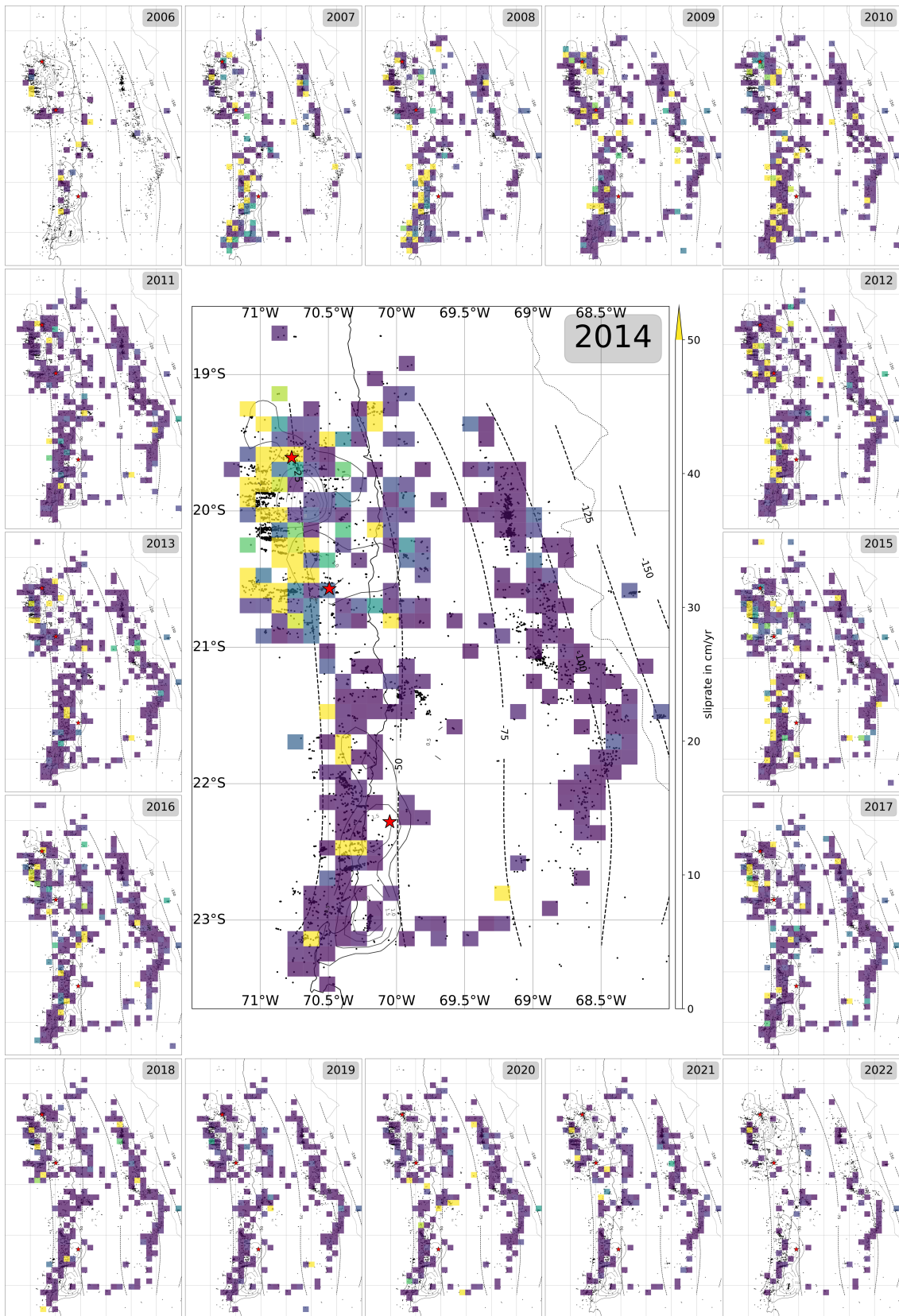


Figure 6 Yearly averaged slip-rate maps for 2006–2022. The year is indicated in the upper right corner of each subplot. Slip-rates are averaged for all RES in a given cell. No spatial smoothing is applied between cells. Highest slip-rates are found up-dip of the 2007 M_w 7.7 Tocopilla event in the years 2007 to 2008 and up-dip of the 2014 M_w 8.1 Iquique event in the years 2014 to 2018. The central map shows the year 2014. The red stars indicate the $M > 7$ event epicenters. Their coseismic slip contours are underlain (Schurr et al., 2012, 2014; Duputel et al., 2015). For all maps, all RE sequences with catalog distances of less than 15 km to the plate interface were used without further selection (black small dots). In contrast to the shallower part of the interface, which undergoes strong spatio-temporal variations, the deeper seismic band (around 69° , about 100 km depth) shows low slip-rates. The plate convergence rate of North Chile is on average 6.7 cm/yr. Larger images of the individual maps are shown in the supplement Figures S11–S15.

ated to creeping faults. These series often show very high event rates in a relatively short time period, hence they should bear the bu- label. We find them located within the crust of the upper plate (tectonic class UP) at shallow to medium crustal depths. They stick out in the slip vs. time plots because of their abnormally high slip-rates. Examples are the series number 93, 89, and 680, having 137, 29, and 29 events within only a few days, respectively. Their corresponding slip histories can be seen in the supplement Figures S4–S9. A second atypical group is comprised of repeater sequences with very high event counts. Figure S9 illustrates the 11 series that consist of at least 40 members. The computed cumulative slip of these groups would be considerably above the expected long term loading rates. Specific local features such as transient high fluid pressure or the stress redistribution effect of a nearby large earthquake could provide an explanation for the temporarily increased slip accumulation in regions of otherwise low loading rates. Alternatively, the multiplets may indicate the activation of adjacent rather than overlapping fault patches. A similar explanation may also apply to the group of repeated burst (rb) type repeater sequences. Examples are the groups 29 or 1669 (cf. Figures S8 & S9). A more detailed analysis, involving careful relocation and individual source parameter estimation, would be necessary to better resolve the source processes of these event groups. This task is beyond the scope of this work.

In the following, we use our new repeater catalog to compute a time resolved slip-rate map of the plate interface for the entire study region, assuming that these repeater groups are indeed indicative for local slip at the plate interface, which we treat here as one single fault. First, we select RE sequences with a maximal distance of 15 km to the plate interface. For each RE sequence, the slip between each pair of subsequent events is divided by their inter-event time to estimate the slip-rate for the corresponding time period. These slip-rate values are assigned to each month between the first and last member of a series. In case of multiple events in a given month, the slip rates are averaged. Next, the monthly slip rates are averaged with those of other neighboring series on a regular spatial grid. The results can be displayed for a given time frame, from one month to multiple years. Exemplarily, Figure 6 shows the yearly average slip-rates for Northern Chile for the years 2006 to 2022. It illustrates the large variability of slip in both space and time. In general, deep-seated RES, located in the intermediate depth band, seem to exhibit low slip rates, with few exceptions. This is a contrast to the statistics of the normal catalogued seismicity, which exhibits highest seismic activity at intermediate depths (Sippl et al., 2023a). The slip rates of the shallow parts of the plate-interface show strong correlation to the occurrence of the large Tocopilla and Iquique earthquakes. In particular, the RE sequences located updip of the main slip patches of the megathrust events exhibit very high yearly averaged slip-rates which decay over several years and appear to depend on the distance to the coseismic high slip patches. Similar observations have been made for repeaters in the vicinity of large

earthquakes in other world regions (e.g., Chen et al., 2010; Chalumeau et al., 2021; Waldhauser and Schaff, 2021).

We plot the slip vs. time curves for all repeater families in the electronic supplement (Figures S4–S9) to illustrate the large variability of repeater recurrence variants. The importance of the 2007 $M_w 7.7$ Tocopilla and in particular the 2014 $M_w 8.1$ Iquique earthquakes on the occurrence of the observed RE series in the region is clearly evident in these figures. Additionally, Figures S11–S15 show an increased-size version of the slip distribution snapshots from Figure 6.

5 Conclusions

We construct a repeating earthquake catalog for the subduction zone in Northern Chile between 18°S and 24°S in the time period from late 2006 to the end of 2024. The catalog comprises 10 684 events grouped into 3153 repeater series. We use a template matching algorithm which scans the continuous seismic waveform data provided by the permanent IPOC network in order to identify repeating events. This computationally expensive approach significantly improves the completeness of the investigated repeater series, compared to waveform cross-correlation of only the earthquakes reported in the IPOC catalog (Sippl et al., 2023a) which we find to contain about half of all identified repeaters.

In general, the catalog describes a considerable spatial and temporal variety of recurrence behavior of repeater series in Northern Chile. We observe repeaters along the interface of the subducting Nazca slab, for intraslab seismicity at intermediate depth and within the crust of the upper plate. REs at the interface indicate strong afterslip in the regions of the two largest megathrust earthquakes, the 2007 $M_w 7.7$ Tocopilla event and the 2014 $M_w 8.1$ Iquique event.

We compute a first time-resolved map of the slip rates at the plate interface for the time period 2006 to 2023.

The reported catalog lists all obtained repeating events and describes their associated repeater families, including a classification of their recurrence behavior type, their tectonic class and several parameters such as magnitudes, average locations, slip, observation period and coefficient of variation. We estimate that this work provides a valuable basis for future research on repeating earthquakes and helps to contribute to a better understanding of the dynamics of the entire subduction zone and the earthquake cycle of large events.

Acknowledgements

We thank Blandine Gardonio and an anonymous reviewer for their comments which helped improve the article. JF was funded by the German Science Foundation (DFG), project numbers FO 1325/3-1.

Data and code availability

The repeater catalog is made available permanently at <https://doi.org/10.5281/zenodo.14770509>. It consists of

three files: 1) the list of repeating earthquakes with all additional parameters as computed in this study, 2) the list of mining events, that fulfill the repeater identification requirements but bear the label mining, and 3) the list of event pairs that have been used to construct the repeater groups including the station information and cross correlation values. The Northern Chile seismic catalog (Sippl et al., 2023b) is available at <https://doi.org/10.5880/GFZ.4.1.2023.004>.

The template matching code is available in static form at <https://doi.org/10.5880/fidgeo.2023.024> and in a maintained version under <https://github.com/RensHofman/SeismicMatch>.

Further processing and visualization was performed in python 3.7 using numpy (Harris et al., 2020) v1.21.6, pandas (The pandas development team, 2025) v1.3.4, obspy (Beyreuther et al., 2010) v.1.2.2, cupy (Okuta et al., 2017) v.11, matplotlib (Hunter, 2007) v3.5.1 & cartopy (Met Office, 2010-2015) v0.20.2.

Competing interests

The authors declare that they have no competing interests.

References

- Beyreuther, M., Barsch, R., Krischer, L., Megies, T., Behr, Y., and Wassermann, J. ObsPy: A Python Toolbox for Seismology. *Seismological Research Letters*, 81(3):530–533, May 2010. doi: [10.1785/gssrl.81.3.530](https://doi.org/10.1785/gssrl.81.3.530).
- Chalumeau, C., Agurto-Detzel, H., De Barros, L., Charvis, P., Galve, A., Rietbrock, A., Alvarado, A., Hernandez, S., Beck, S., Font, Y., Hoskins, M. C., León-Ríos, S., Meltzer, A., Lynner, C., Rolandone, F., Nocquet, J., Régnier, M., Ruiz, M., Soto-Cordero, L., Vaca, S., and Segovia, M. Repeating Earthquakes at the Edge of the Afterslip of the 2016 Ecuadorian MW7.8 Pedernales Earthquake. *Journal of Geophysical Research: Solid Earth*, 126(5), May 2021. doi: [10.1029/2021jb021746](https://doi.org/10.1029/2021jb021746).
- Chen, K. H., Nadeau, R. M., and Rau, R.-J. Characteristic repeating earthquakes in an arc-continent collision boundary zone: The Chihshang fault of eastern Taiwan. *Earth and Planetary Science Letters*, 276(3–4):262–272, Dec. 2008. doi: [10.1016/j.epsl.2008.09.021](https://doi.org/10.1016/j.epsl.2008.09.021).
- Chen, K. H., Bürgmann, R., Nadeau, R. M., Chen, T., and Lapusta, N. Postseismic variations in seismic moment and recurrence interval of repeating earthquakes. *Earth and Planetary Science Letters*, 299(1–2):118–125, Oct. 2010. doi: [10.1016/j.epsl.2010.08.027](https://doi.org/10.1016/j.epsl.2010.08.027).
- Chen, K. H., Furumura, T., Rubinstein, J., and Rau, R.-J. Observations of changes in waveform character induced by the 1999 Mw7.6 Chi-Chi earthquake: HEALING OF SUBSURFACE DAMAGE. *Geophysical Research Letters*, 38(23), Dec. 2011. doi: [10.1029/2011gl049841](https://doi.org/10.1029/2011gl049841).
- Duputel, Z., Jiang, J., Jolivet, R., Simons, M., Rivera, L., Ampuero, J., Riel, B., Owen, S. E., Moore, A. W., Samsonov, S. V., Ortega Culaciati, F., and Minson, S. E. The Iquique earthquake sequence of April 2014: Bayesian modeling accounting for prediction uncertainty. *Geophysical Research Letters*, 42(19):7949–7957, Oct. 2015. doi: [10.1002/2015gl065402](https://doi.org/10.1002/2015gl065402).
- Folesky, J., Pennington, C. N., Kummerow, J., and Hofman, L. J. A Comprehensive Stress Drop Map From Trench to Depth in the Northern Chilean Subduction Zone. *Journal of Geophysical Research: Solid Earth*, 129(1), Jan. 2024. doi: [10.1029/2023jb027549](https://doi.org/10.1029/2023jb027549).
- Gao, D., Kao, H., and Wang, B. Misconception of Waveform Similarity in the Identification of Repeating Earthquakes. *Geophysical Research Letters*, 48(13), July 2021. doi: [10.1029/2021gl092815](https://doi.org/10.1029/2021gl092815).
- GFZ German Research Centre For Geosciences and Institut Des Sciences De L'Univers-Centre National De La Recherche CNRS-INSU. IPOC Seismic Network, 2006. doi: [10.14470/PK615318](https://doi.org/10.14470/PK615318).
- Hanks, T. C. and Kanamori, H. A moment magnitude scale. *Journal of Geophysical Research: Solid Earth*, 84(B5):2348–2350, May 1979. doi: [10.1029/jb084ib05p02348](https://doi.org/10.1029/jb084ib05p02348).
- Harris, C. R., Millman, K. J., van der Walt, S. J., Gommers, R., Virtanen, P., Cournapeau, D., Wieser, E., Taylor, J., Berg, S., Smith, N. J., Kern, R., Picus, M., Hoyer, S., van Kerkwijk, M. H., Brett, M., Haldane, A., del Río, J. F., Wiebe, M., Peterson, P., Gérard-Marchant, P., Sheppard, K., Reddy, T., Weckesser, W., Abbasi, H., Gohlke, C., and Oliphant, T. E. Array programming with NumPy. *Nature*, 585(7825):357–362, Sept. 2020. doi: [10.1038/s41586-020-2649-2](https://doi.org/10.1038/s41586-020-2649-2).
- Hofman, L. J., Kummerow, J., Cesca, S., Group, A.-S.-D. W., et al. A new seismicity catalogue of the eastern Alps using the temporary Swath-D network. *Solid Earth*, 14(10):1053–1066, Oct. 2023. doi: [10.5194/se-14-1053-2023](https://doi.org/10.5194/se-14-1053-2023).
- Hughes, L., Chamberlain, C. J., Townend, J., and Thomas, A. M. A Repeating Earthquake Catalog From 2003 to 2020 for the Raukumara Peninsula, Northern Hikurangi Subduction Margin, New Zealand. *Geochemistry, Geophysics, Geosystems*, 22(5), Apr. 2021. doi: [10.1029/2021gc009670](https://doi.org/10.1029/2021gc009670).
- Hunter, J. D. Matplotlib: A 2D Graphics Environment. *Computing in Science & Engineering*, 9(3):90–95, 2007. doi: [10.1109/mcse.2007.55](https://doi.org/10.1109/mcse.2007.55).
- Igarashi, T. Spatial changes of inter-plate coupling inferred from sequences of small repeating earthquakes in Japan. *Geophysical Research Letters*, 37(20), Oct. 2010. doi: [10.1029/2010gl044609](https://doi.org/10.1029/2010gl044609).
- Igarashi, T. Catalog of small repeating earthquakes for the Japanese Islands. *Earth, Planets and Space*, 72(1), May 2020. doi: [10.1186/s40623-020-01205-2](https://doi.org/10.1186/s40623-020-01205-2).
- Igarashi, T., Matsuzawa, T., and Hasegawa, A. Repeating earthquakes and interplate aseismic slip in the northeastern Japan subduction zone. *Journal of Geophysical Research: Solid Earth*, 108(B5), May 2003. doi: [10.1029/2002jb001920](https://doi.org/10.1029/2002jb001920).
- Kato, A., Fukuda, J., Kumazawa, T., and Nakagawa, S. Accelerated nucleation of the 2014 Iquique, Chile Mw 8.2 Earthquake. *Scientific Reports*, 6(1), Apr. 2016. doi: [10.1038/srep24792](https://doi.org/10.1038/srep24792).
- Matsuzawa, T., Uchida, N., Igarashi, T., Okada, T., and Hasegawa, A. Repeating earthquakes and quasi-static slip on the plate boundary east off northern Honshu, Japan. *Earth, Planets and Space*, 56(8):803–811, June 2014. doi: [10.1186/bf03353087](https://doi.org/10.1186/bf03353087).
- Meng, L., Huang, H., Bürgmann, R., Ampuero, J. P., and Strader, A. Dual megathrust slip behaviors of the 2014 Iquique earthquake sequence. *Earth and Planetary Science Letters*, 411:177–187, Feb. 2015. doi: [10.1016/j.epsl.2014.11.041](https://doi.org/10.1016/j.epsl.2014.11.041).
- Menke, W. Using waveform similarity to constrain earthquake locations. *Bulletin of the Seismological Society of America*, 89(4): 1143–1146, Aug. 1999. doi: [10.1785/bssa0890041143](https://doi.org/10.1785/bssa0890041143).
- Met Office. Cartopy: a cartographic python library with a Matplotlib interface. Exeter, Devon, 2010–2015. <https://scitools.org.uk/cartopy>.
- Nadeau, R. M. and Johnson, L. R. Seismological studies at Parkfield VI: Moment release rates and estimates of source parameters for small repeating earthquakes. *Bulletin of the Seismological Society of America*, 88(3):790–814, June 1998. doi: [10.1785/bssa088003790](https://doi.org/10.1785/bssa088003790).

- ssa0880030790.
- Okuta, R., Unno, Y., Nishino, D., Hido, S., and Loomis, C. CuPy: A NumPy-Compatible Library for NVIDIA GPU Calculations. In *Proceedings of Workshop on Machine Learning Systems (LearningSys) in The Thirty-first Annual Conference on Neural Information Processing Systems (NIPS)*, 2017. http://learningsys.org/nips17/assets/papers/paper_16.pdf.
- Rubinstein, J. L., Uchida, N., and Beroza, G. C. Seismic velocity reductions caused by the 2003 Tokachi-Oki earthquake. *Journal of Geophysical Research: Solid Earth*, 112(B5), May 2007. doi: 10.1029/2006jb004440.
- Schurr, B., Asch, G., Rosenau, M., Wang, R., Oncken, O., Barrientos, S., Salazar, P., and Vilote, J. The 2007 M7.7 Tocopilla northern Chile earthquake sequence: Implications for along-strike and downdip rupture segmentation and megathrust frictional behavior. *Journal of Geophysical Research: Solid Earth*, 117(B5), May 2012. doi: 10.1029/2011jb009030.
- Schurr, B., Asch, G., Hainzl, S., Bedford, J., Hoechner, A., Palo, M., Wang, R., Moreno, M., Bartsch, M., Zhang, Y., Oncken, O., Tilmann, F., Dahm, T., Victor, P., Barrientos, S., and Vilote, J.-P. Gradual unlocking of plate boundary controlled initiation of the 2014 Iquique earthquake. *Nature*, 512(7514):299–302, Aug. 2014. doi: 10.1038/nature13681.
- Sippl, C., Schurr, B., Asch, G., and Kummerow, J. Seismicity Structure of the Northern Chile Forearc From >100,000 Double-Difference Relocated Hypocenters. *Journal of Geophysical Research: Solid Earth*, 123(5):4063–4087, May 2018. doi: 10.1002/2017jb015384.
- Sippl, C., Schurr, B., Münchmeyer, J., Barrientos, S., and Oncken, O. The Northern Chile forearc constrained by 15 years of permanent seismic monitoring. *Journal of South American Earth Sciences*, 126:104326, June 2023a. doi: 10.1016/j.jsames.2023.104326.
- Sippl, C., Schurr, B., Münchmeyer, J., Barrientos, S., and Oncken, O. Catalogue of Earthquake Hypocenters for Northern Chile from 2007–2021 using IPOC (plus auxiliary) seismic stations, 2023b. doi: 10.5880/GFZ.4.1.2023.004.
- Soto, H., Sippl, C., Schurr, B., Kummerow, J., Asch, G., Tilmann, F., Comte, D., Ruiz, S., and Oncken, O. Probing the Northern Chile Megathrust With Seismicity: The 2014 M8.1 Iquique Earthquake Sequence. *Journal of Geophysical Research: Solid Earth*, 124(12):12935–12954, Dec. 2019. doi: 10.1029/2019jb017794.
- The pandas development team. pandas-dev/pandas: Pandas, 2025. doi: 10.5281/ZENODO.3509134.
- Uchida, N. Detection of repeating earthquakes and their application in characterizing slow fault slip. *Progress in Earth and Planetary Science*, 6(1), May 2019. doi: 10.1186/s40645-019-0284-z.
- Uchida, N. and Bürgmann, R. Repeating Earthquakes. *Annual Review of Earth and Planetary Sciences*, 47(1):305–332, May 2019. doi: 10.1146/annurev-earth-053018-060119.
- Uchida, N. and Bürgmann, R. A Decade of Lessons Learned from the 2011 Tohoku-Oki Earthquake. *Reviews of Geophysics*, 59(2), May 2021. doi: 10.1029/2020rg000713.
- Waldhauser, F. and Schaff, D. P. A Comprehensive Search for Repeating Earthquakes in Northern California: Implications for Fault Creep, Slip Rates, Slip Partitioning, and Transient Stress. *Journal of Geophysical Research: Solid Earth*, 126(11), Nov. 2021. doi: 10.1029/2021jb022495.

The article *A repeating earthquake catalog for Northern Chile* © 2025 by Jonas Folesky is licensed under CC BY 4.0.